


# Substantial genetic divergence and lack of recent gene flow support cryptic speciation in a colour polymorphic bumble bee (*Bombus bifarius*) species complex

GUILLAUME GHISBAIN<sup>1</sup>, JEFFREY D. LOZIER<sup>2</sup>,  
SARTHOK RASIQUE RAHMAN<sup>3</sup>, BRIANA D. EZRAY<sup>4</sup>,  
LI TIAN<sup>3</sup>, JONAH M. ULMER<sup>4</sup>, SAM D. HERAGHTY<sup>2</sup>,  
JAMES P. STRANGE<sup>5,6</sup>, PIERRE RASMONT<sup>1</sup>  
and HEATHER M. HINES<sup>3,4</sup> 

<sup>1</sup>Laboratory of Zoology, Research Institute of Biosciences, University of Mons, Mons, Belgium, <sup>2</sup>Department of Biological Sciences, The University of Alabama, Tuscaloosa, AL, USA, <sup>3</sup>Department of Biology, The Pennsylvania State University, University Park, PA, USA, <sup>4</sup>Department of Entomology, The Pennsylvania State University, University Park, PA, USA, <sup>5</sup>United States Department of Agriculture-Agricultural Research Services, Pollinating Insects-Biology, Management, and Systematics Research Laboratory, Logan, UT, USA and <sup>6</sup>Department of Entomology, The Ohio State University, Columbus, OH, USA

**Abstract.** Phenotypic polymorphism can constitute an inherent challenge for species delimitation. This issue is exemplified in bumble bees (*Bombus*), where species can exhibit high colour variation across their range, but otherwise exhibit little morphological variation to distinguish them from close relatives. We examine the species status of one of the most abundant North American bumble bees, *Bombus bifarius* Cresson, which historically comprised two major taxa, *bifarius* s.s. and *nearcticus*. These lineages are recognized primarily by red and black variation in their mid-abdominal coloration; however, a continuum from black (*nearcticus*) to red (*bifarius* s.s.) variation has led to their historic synonymization. Integrating mitochondrial and nuclear data and whole-genome sequencing, we reveal a high level of both mitochondrial and nuclear divergence delimiting two morphologically cryptic species – the red *bifarius* s.s. and the colour-variable (black to red) *nearcticus*. Population genomic analysis supports an absence of recent genomic admixture and a strong population structure between the two clades, even in sympatry. Species distribution models predict partially differentiated niches between the genetically inferred clades with annual precipitation being a leading differentiating variable. The *bifarius* s.s. lineage also occupies significantly higher elevations, with regions of sympatry being among the highest elevations in *nearcticus*. Our data also support a subspecies-level divergence between the broadly distributed *nearcticus* and the island population *vancouverensis*. In this paper, we formally recognize the two species, *Bombus bifarius* Cresson and *Bombus vancouverensis* Cresson, the latter including the subspecies *B. vancouverensis vancouverensis* **comb.n.** and *B. vancouverensis nearcticus* **comb.n.**, with *vancouverensis* the name bearer due to year priority.

## Introduction

The processes generating and maintaining genetic and phenotypic diversity in polymorphic organisms are of great interest in evolutionary biology. Such polymorphic populations are

useful for revealing the complex interplay of drift, admixture and selection in shaping phenotypic diversity. However, they can present substantial challenges in species delimitation. For example, some polymorphic species may lack genetic structure, whereas others may contain multiple ‘cryptic’ species masked by a lack of discrete morphological, behavioural and/or ecological characters (Bickford *et al.*, 2007; Pfenninger & Schwenk, 2007; Murray *et al.*, 2008). Resolving the species status of such

Correspondence: Department of Biology, The Pennsylvania State University, University Park, PA 16801, USA. E-mail: hhm19@psu.edu

lineages is necessary for understanding the origins and evolution of such variation, and is critical for assigning accurate taxonomy, conducting biodiversity assessments and aiding their conservation (May, 1988; Bickford *et al.*, 2007).

Bumble bees (Hymenoptera: Apoidea: genus *Bombus* Latreille) are an emerging model system for understanding patterns of complex species diversity (Woodard *et al.*, 2015). The ~260 *Bombus* species recognized worldwide (Williams, 1998) occur mostly in temperate areas of the Northern Hemisphere (e.g. Corbet *et al.*, 1991; Memmott *et al.*, 2004; Hegland & Totland, 2008), where they contribute to ecosystem services through pollination of both wild plants and crops. These vital ecosystem services (Kremen *et al.*, 2002; Velthuis & Van Doorn, 2006) are under threat, as bumble bee declines have been recognized worldwide (Williams & Osborne, 2009; Cameron *et al.*, 2011; Kerr *et al.*, 2015). Ultimately, the conservation of these important pollinators depends on accurate species-level identification.

Species delimitation has been challenging in bumble bees, as they have been considered ‘morphologically monotonous’ (Michener, 2000), often exhibiting only minor character differences such as details of head puncturing and male genitalia morphology to diagnose closely related species. By contrast, coloration of thoracic and abdominal setae can be highly variable, leading to a historical focus on colour traits for species diagnosis. Colour patterns, however, can be poor traits for diagnosis in bumblebees (Carolan *et al.*, 2012; Hines & Williams, 2012; Koch *et al.*, 2018). One of the major reasons for this colour variation is Müllerian mimicry, which has driven many *Bombus* species towards nearly identical colour patterns within a geographical region, while promoting diverse colour forms within species across their distributions (Williams, 2007). Such high variation and convergence, the general unreliability of colour traits, and the lack of morphological characters on which to base species decisions has led to many cases of taxonomic misclassification (Ellis *et al.*, 2006; Bertsch, 2009; Koch *et al.*, 2018), contributing to bumble bees being one of the most highly synonymized lineages (Williams, 1998).

Although definitions of species can vary (Mayr, 1961; De Queiroz, 2007; Woodard *et al.*, 2015), a practical definition which we apply here is to consider them as independently evolving lineages (de Queiroz, 2007) with little to no evidence of gene flow. In practice, examining multiple lines of evidence (e.g. Lecocq *et al.*, 2015; Martinet *et al.*, 2019; Williams *et al.*, 2019) is optimal for recognizing whether character states are discrete between lineages, and are thus evolving separately. For example, mitochondrial DNA sequence data can yield more resolved and discrete histories given a lack of recombination, haploidy and maternal inheritance; however, mitochondrial genes can lead to false interpretations because of introgression, selection, sex-biased histories and historical population isolation. Nuclear sequence data, although confounded by incomplete lineage sorting, provide an independent signature of population history that is better at revealing recent and ancient patterns of introgression. Genome-wide sequencing data are particularly informative about the extent of admixture by revealing whether any possible introgression is widespread throughout the genome, restricted

to certain gene regions, or largely absent. Integrated approaches combining morphology, nuclear and mitochondrial sequences, and/or chemical data, are common for bumble bee species delimitation (e.g. Lecocq *et al.*, 2015; Martinet *et al.*, 2019; Williams *et al.*, 2019).

In North America, one of the most taxonomically confounding species is *Bombus bifarius* Cresson (subgenus *Pyrobombus* Dalla Torre), a widespread and abundant taxon distributed in western mountain ranges from the American Southwest to Alaska. The species displays a striking range of colour patterns across its distribution, resulting in various subspecific epithets for its phenotypic variants (Stephen, 1957). The main morphotypes were originally described as separate species during early descriptions of North American fauna (Cresson, 1878; Handlirsch, 1888) and have since been synonymized as subspecies given their shared morphologies and continuous gradation in colour variation (e.g. Stephen, 1957; Williams, 1998). Two primary subspecies are recognized: *Bombus bifarius nearcticus* (henceforth referred to as *nearcticus*), having metasomal T2–3 ranging from all black to mostly red and occurring in the western part of the distribution and *Bombus bifarius bifarius* (henceforth referred to as *bifarius* s.s.), with T2–3 largely red and dominating in the eastern part of the species range (Fig. 1; Stephen, 1957; Lozier *et al.*, 2013; Ezray *et al.*, 2019). Aside from differences in colour, variation in the terminal male sternite was reported to potentially discriminate these two taxa (Stephen, 1957). A third taxon, *Bombus bifarius vancouverensis* (henceforth referred to as *vancouverensis*), occurs on Vancouver Island and surrounding islands of the Salish Sea (Fig. 1), exhibiting distinctive features of having whiter setae on the thorax, and largely red T2+3 segments similar to disjunct eastern *bifarius* populations.

Previous studies have investigated population dynamics of the *B. bifarius* species complex (i.e. including *bifarius* s.s., *nearcticus* and *vancouverensis*, henceforth referred to as *Bombus bifarius* s.l.) using multiple genetic methods. Studies using microsatellites and colour pattern have suggested the presence of ongoing gene flow consistent with genetically heterogeneous, but partially connected conspecific populations (Lozier *et al.*, 2011, 2013). Subsequent genomic analyses of transcriptome and double digest restriction enzyme associated DNA sequencing (ddRADSeq) have cast doubt on existing taxonomy, suggesting substantial divergence without gene flow between red *bifarius* s.s. and black to intermediately coloured *nearcticus* lineages (Lozier *et al.*, 2016a). These studies raise the possibility that *B. bifarius* s.l. may represent a complex of phenotypically polymorphic cryptic species.

In this paper, we rigorously assess the specific status of *B. bifarius* s.l. by examining patterns of gene flow and lineage isolation among all three lineages using a combined mitochondrial gene and nuclear genomic approach. We sample the mitochondrial barcode (*COI*) marker from individuals across the species range to determine patterns of population structure, and utilize whole-genome sequencing of representative individuals, along with more abundant taxon sampling of specific informative nuclear markers, to test for genomic admixture in regions of allopatry and sympatry. We then use occurrence data and

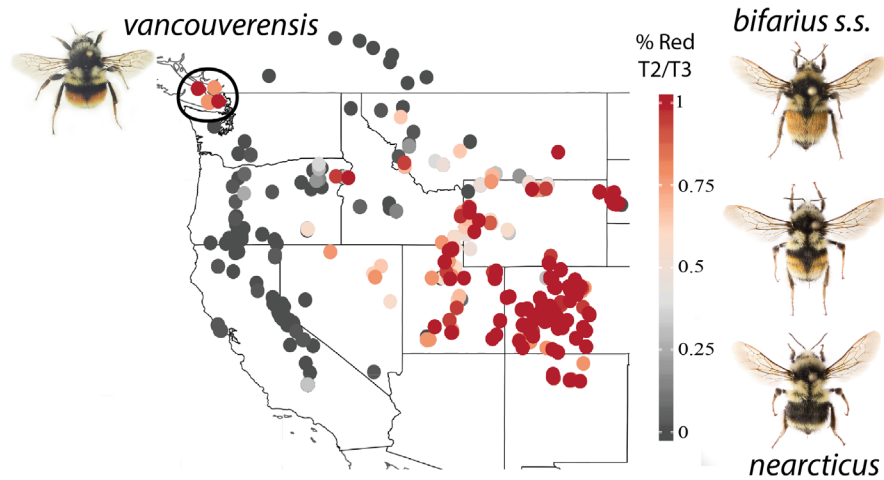


**Fig. 1.** Distribution of colour forms in *Bombus bifarius* s.l. with colour patterns and regions assigned to historically recognized taxa names indicated. Assignment of intermediate colour forms to species was not well-defined historically. % Red T2/T3 = the percentage of the second and third metasomal tergites with red-orange setal coloration. Distribution data based on Ezray *et al.* (2019). [Colour figure can be viewed at [wileyonlinelibrary.com](http://wileyonlinelibrary.com)].

bioclimatic variables to determine the role of ecological niche in the inferred species distributions and assess whether defined genetic lineages can be further demarcated with morphological features. We finally assess the taxonomic status of the lineages *bifarius* s.s., *nearcticus*, and *vancouverensis* considering available type material and their original descriptions.

## Material and methods

### Phylogenetic inference of mitochondrial COI

**Sampling.** Specimens were obtained from across the *B. bifarius* s.l. distribution, including Alaska (AK, USA), Yukon (YT, Canada), and the western United States (WA, OR, CA, ID, WY, UT and CO) (N=119; Appendix S1), and were collected within the last 10 years. Sampling intentionally covered a large part of the colour forms displayed by the group, from the bright, fully red-banded Eastern specimens (*bifarius* s.s.), through diverse intermediate forms, to the extensively black ones (*nearcticus*), and also included three exemplars of *vancouverensis* from the San Juan Islands, WA. Most specimens used were directly transferred into 100% ethanol at  $-20^{\circ}\text{C}$  after collecting, whereas others were mounted and dried.

**DNA preparation, amplification and sequencing for COI.** Total DNA was extracted from the hind legs of the specimens using E.Z.N.A. Tissue DNA Kits (Omega Bio-tek, Norcross, GA, USA). Legs were crushed and digested with protease K for 3.5 hours at  $55^{\circ}\text{C}$  before column extraction, following the manufacturer's protocol with a single, final elution in  $50\mu\text{L}$  of elution buffer. Samples were individually checked for both purity (NanoDrop One<sup>c</sup>, Thermo Fischer Scientific) and integrity (1% agarose electrophoresis gel) before amplification. Polymerase chain reaction (PCR) amplifications were carried out (Hot Start *Taq* 2x Master Mix, NEB) on a commonly used

gene for species delimitation in bumble bees (e.g., Duennes *et al.*, 2012; Williams *et al.*, 2012) and other insects: the mitochondrial barcode fragment of the cytochrome oxidase I (*COI*). We amplified ~640 bp of *COI* using universal primers LCO1490 (5'-GGTCAACAATCATAAAGATATTGG-3') and HC02198 (5'-TAAACTTCAGGGTGACCAAAAAATCA-3') (Folmer *et al.*, 1994) with the amplification conditions as follows: initial denaturing at  $94^{\circ}\text{C}$  for 2 min, a first cycle of 30 s at  $94^{\circ}\text{C}$ , 40 s at  $45^{\circ}\text{C}$ , 1 min at  $72^{\circ}\text{C}$ , followed by 35 cycles of 30 s at  $94^{\circ}\text{C}$ , 40 s at  $49^{\circ}\text{C}$ , 1 min at  $72^{\circ}\text{C}$ , before final elongation of 10 min at  $72^{\circ}\text{C}$ . DNA from all amplified samples was enzymatically purified using ExoSAP-IT<sup>TM</sup> (Thermo Fischer Scientific) followed by Sanger sequencing (Genomic Core Facility, Pennsylvania State University, PA, USA).

**COI phylogenetic inference and haplotype network.** We constructed a *COI* Bayesian phylogeny of 119 newly sequenced individuals along with sequences of 48 additional *B. bifarius* s.l. individuals from all three lineages obtained from GenBank (<https://www.ncbi.nlm.nih.gov/genbank/>). Sequences were selected from GenBank to include representative individuals from each sampled locality and only sequences with nearly complete *COI* data in the sequenced interval. To examine the placement of each lineage relative to the closest extant relatives, we also included exemplar *COI* sequences of the closest relatives (Cameron *et al.*, 2007) to *B. bifarius* s.l., including *Bombus ephippiatus*, *Bombus impatiens*, *Bombus huntii*, *Bombus ternarius* and *Bombus vosnesenskii*, along with the slightly more distant *Bombus melanopygus* as an outgroup, using either newly sequenced individuals or sequences from GenBank (Appendix S1). Comparative 'Percent Identity' values in GenBank were used to confirm that these exemplars were typical representatives of the diversity of *COI* sequences in their respective species clades. *COI* sequences were edited manually and aligned in GENEIOUS v8.1.9 (Biomatters, <http://www.geneious.com>), with ends trimmed to remove missing

data to yield a 562-bp aligned fragment. The best available model for our *COI* data according to the Bayesian Information Criterion (BIC) obtained from MEGA X (v10.0.5; Kumar *et al.*, 2018) is GTR+I+ $\Gamma$ . We performed Bayesian inference under this model using MRBAYES 3.2.6 (Ronquist & Huelsenbeck, 2003) analyzed in the CIPRES Science Gateway v3.3 servers (<https://www.phylo.org>) with four independent runs, four chains, 15 million generations and sampling trees every 1000 generations. We assessed convergence through examining likelihood plots (confirming stationarity) and convergence statistics in MRBAYES 3.2.6 and ESS values in TRACER 1.7.1 (Rambaut *et al.*, 2018), which led us to conservatively discard the first 25% of the trees as burn-in for all runs to obtain a majority-rule 50% consensus tree. This tree was run through the Poisson-Tree-Process procedure (PTP; Zhang *et al.*, 2013), which applies coalescent models to designate optimal species assignments from an input tree, using the bPTP server (<https://species.h-its.org/>) and applying default PTP options. We also constructed a haplotype network for the 119 newly sequenced individuals using a 584-bp fragment of *COI* with no missing data. The network was constructed using the median-joining method in NETWORK 5.0.0.3 (<http://www.fluxus-engineering.com/>) and haplotypes were mapped geographically. Sequence alignments are available at Dryad (doi.org/10.5061/dryad.7d7wm37r9), and newly obtained sequences on GenBank (Accession numbers MN781411-MN781539).

#### Genomic tests of admixture

**Sampling.** To assess population structure and admixture, we performed whole genome sequencing on 21 bee specimens (Appendix S1) that represent the two major lineages inferred from our mitochondrial data ('*nearcticus*-clade' and '*bifarius*-clade'), thus enabling comparison between mitochondrial and genomic signatures. Sampling included five mostly black *nearcticus*-clade haploid males from different locations in the western United States (CA, OR; *nearcticus*-West), one diploid queen representing the historical *vancouverensis* lineage from within the *nearcticus*-clade (San Juan Island, WA), four mostly red *bifarius* s.s.-clade individuals from separate locations in CO and eastern UT (three diploid workers, one haploid male), and 11 mostly red *nearcticus*-clade males from several geographically intermediate locations in the central Rockies (UT and WY; *nearcticus*-Central). By sampling *nearcticus* populations both distant and close to *bifarius* s.s. populations, we can test for signatures of admixture along a geographical gradient. The more abundant sampling of central *nearcticus* allows more individuals to be examined for signs of admixture in the possible contact zone. This sampling included individuals from both lineages (one each) collected together at the same site in the eastern Uinta Mountains (Utah, USA) thus allowing direct assessment of whether gene flow is occurring in sympatry.

**Genomic sequencing and variant calling.** Leg or thoracic muscle tissue was extracted from the male samples, previously kept frozen or in ~90% ethanol at  $-20^{\circ}\text{C}$ , using an E.Z.N.A.

DNA extraction kit run with standard protocols. Samples were prepared for sequencing using an Illumina TruSeq DNA Nano library construction kit following standard protocols. DNA from the diploid Colorado samples was extracted with Qiagen (Venlo, the Netherlands) DNeasy kits (with RNase treatment) following modifications in Lozier (2014). Dual-indexed Illumina libraries for the diploid samples were prepared by HudsonAlpha Institute for Biotechnology Genome Services Lab (Huntsville, AL USA) for *CO bifarius* s.s.-clade bees or Psomagen, Inc. (Rockville, MD) for the *vancouverensis* specimen. Whole-genome sequencing for haploid samples ( $n = 17$ ) was performed using an Illumina HiSeq 2500 sequencer to generate  $2 \times 150$ -bp paired-end read libraries at Pennsylvania State University Genomics Core Facility. Diploid samples ( $n = 4$ ) were sequenced ( $2 \times 150$ -bp paired end reads) on an Illumina HiSeq X (HudsonAlpha) or a NovaSeq6000 S4 (Psomagen). After initial quality control assessment of raw sequencing reads performed with FASTQC v0.11.7 (Andrews, 2010), appropriate quality control on the raw reads was conducted using TRIMMOMATIC v0.38 (Bolger *et al.*, 2014) to remove low-quality bases (SLIDINGWINDOW:4:30 LEADING:3 TRAILING:3), clip adapters (ILLUMINACLIP:adapters.fa:2:30:5) and discard reads  $<36$  bp (MINLEN:36). Post-QC reads were aligned to the published genome assembly of closely related *B. impatiens* (NCBI GenBank Assembly GCA\_000188095.3, BIMP\_2.1; Sadd *et al.*, 2015) using BWA v0.7.17, utilizing the BWA-mem algorithm with default parameters (Li & Durbin, 2009). Post-processing of aligned reads was conducted in SAMTOOLS v1.8 (Li *et al.*, 2009) and PICARD TOOLS v1.119 (available at: <http://broadinstitute.github.io/picard/index.html>).

Multi-sample variant calling for haploid samples ( $n = 17$ ) was performed using GATK UNIFIED GENOTyper v3.6 (McKenna *et al.*, 2010; DePristo *et al.*, 2011) following best practices (Van der Auwera *et al.*, 2013) with specific parameters for haploidy [-ploidy 1 -glm single nucleotide polymorphism (SNP) -stand\_call\_conf 25.0]. The variant calling procedure for diploid ( $n = 4$ ) samples was conducted using the same protocol except for diploid designation (-ploidy 2). Variant calling datasets from both procedures were merged using the COMBINE VARIANTS utility in GATK.

We generated two filtered datasets for different genomic analyses. One dataset was used for statistical analyses of individual bee genotypes (e.g. principal components analysis, neighbour-joining analysis, population structure inference), hereafter referred to as the 'individual-level' dataset, that included *bifarius* s.s., *nearcticus*-Central, *nearcticus*-West and the single San Juan Island *vancouverensis* bee ( $n = 21$ ). Filtering of this dataset included allowing a minimum minor allele count of one, requiring a maximum of two alleles, minimum depth per SNP per bee of four, minimum genotype quality 20; we also excluded a small number of sites ( $n = 50\,645$ ) which had any heterozygous sites in haploid samples (erroneous by definition) and any sites with missing data. Finally, we restricted our analyses to the 78 scaffolds with length  $>1$  Mb (total of 154 Mb, 63% of total *B. impatiens* genome length). The final individual-level dataset had 322 605 SNPs.

The second dataset was used for population-level analysis ('population-level' dataset, used to analyze genetic diversity, population differentiation and admixture). This differed from the individual-level dataset in excluding the single *vancouverensis* specimen ( $n = 20$ ). Filters for SNPs included requiring a maximum of two alleles, minimum depth per SNP per bee of four, minimum genotype quality 20, minimum root mean squared mapping quality 40, missing data rate of maximum 20%, and a minimum minor allele count of two, resulting in 426 358 total SNPs.

*Individual-level analysis of genomic relationships.* To infer the relationship among all individuals ( $n = 21$ ), a principal component analysis (PCA) was conducted on the filtered SNP dataset (322 605 SNPs) using the PCA option from the Analysis menu in TASSEL 5 (Bradbury *et al.*, 2007). The first two principal components were plotted using the GGPLOT2 (Wickham, 2016) package in R. A neighbour-joining distance-based tree was constructed from the filtered variant calling data using TASSEL 5 (Bradbury *et al.*, 2007). To infer population structure, sNMF analysis was implemented in R/LEA (Frichot & François, 2015). We removed mixed ploidy by phasing all diploid ( $n = 4$ ) individuals using BEAGLE v4.1 (Browning & Browning, 2007, parameters impute = false window = 10000 overlap = 1000 gprobs = false), effectively treating them as two haploid individuals each. We ran five independent runs at each  $K$ -value ( $K = 1$  to 10) and obtained the optimal number of ancestral population assignments by assessing minimum cross-entropy across all  $K$ -values.

*Population-level analyses of diversity, population structure and admixture.* We used custom bioinformatics scripts by Simon Martin implementing methods from (Martin *et al.*, 2015; Van Belleghem *et al.*, 2017; [http://github.com/simonmartin/genomics\\_general](http://github.com/simonmartin/genomics_general)) to perform genome-wide population genetic analyses on 20 bees and 426 358 SNPs representing population-level samples (*bifarius* s.s., *nearcticus*-West, *nearcticus*-Central). These methods have the advantage of allowing a mixture of haploids and diploids in the sample set. Allele frequencies were estimated at each site using *B. impatiens* as a reference. We calculated nucleotide diversity ( $\pi$ ) within *nearcticus*-West, *nearcticus*-Central and *bifarius* s.s., and the fixation index  $F_{ST}$  and absolute divergence ( $d_{XY}$ ) between group pairs across 100-kb sliding windows across the genome containing at least 100 SNPs, slid by 25 kb per step. Mean and confidence intervals for genome-wide  $\pi$ ,  $F_{ST}$  and  $d_{XY}$  were determined by jack-knifing over the 100-kb blocks using R/BOOTSTRAP.

Analyses of introgression were conducted using the ABBA-BABA framework (Green *et al.*, 2010) with scripts by Simon Martin as above. Most analyses employed a three-population model  $\{(P_1, P_2), P_3, O\}$  where *nearcticus*-West is specified as  $P_1$ , *bifarius* s.s. as  $P_3$  and central *nearcticus*-Central as the hypothesized admixed lineage ( $P_2$ ) (3-Pop model; see Figure S1 for schematic of models examined in this study). Under a history of pure divergence and drift, alleles at polymorphic sites should only be shared by these

populations due to incomplete lineage sorting, which should result in an equal number of SNPs with the derived allele ('B', vs. ancestral allele 'A') shared by *bifarius* s.s. ( $P_3$ ) and either *nearcticus* population ( $P_1$  or  $P_2$ ) and thus ABBA sites equal BABA sites. By contrast, with post-divergence gene flow, it is expected that  $P_3$  and  $P_2$  (the neighbouring Utah *nearcticus* and *bifarius* s.s. populations) would share an excess of nonreference alleles, resulting in an excess of ABBA over BABA sites. Several statistics have been developed to quantify this excess, including Patterson's  $D$  (Green *et al.*, 2010), which is most suitable for examining introgression at the whole-genome level, and the admixture proportion  $f_D$  (Martin *et al.*, 2015), which is more suitable for examining the proportion of admixture at narrower genome windows to identify potentially introgressed chromosomal regions. We report  $D$  and  $f_{DM}$  (Malinsky *et al.*, 2015), a modification of  $f_D$  that is bounded between  $[-1, 1]$  and symmetrically distributed around zero under a null hypothesis of no gene flow, although all ABBA-BABA statistics were highly correlated. In all cases, positive values represent potential introgression between  $P_3$  and  $P_2$  (ABBA > BABA), whereas values of zero are consistent with a model of divergence and drift alone (ABBA = BABA). As above, genome-wide estimates were calculated in nonoverlapping 100-kb blocks, as well as averaged for each scaffold, and significance (95% confidence intervals) of whole-genome estimates was tested using block jack-knifing. In a second analysis (Hybrid-zone model) we used the single *nearcticus*-Central bee with a red phenotype (confirmed by *COI* sequence) collected from within the range of *bifarius* s.s. in the Uinta Mountains of Utah, and tested for hybridization by specifying this sample as  $P_2$ , with other *nearcticus*-Central bees as  $P_1$  and *bifarius* s.s. as  $P_3$ .

We also examined ancestry and potential for recent admixture of populations within the putative hybrid population (*nearcticus*-Central) using an ancestry painting approach (Der Sarkissian *et al.*, 2015; Runemark *et al.*, 2018; scripts from <https://github.com/mmatschiner/> were used to conduct this analysis). First, we extracted SNPs with alternate alleles fixed between *bifarius* s.s. and *nearcticus*-West, using only SNPs with no missing data. The genotypes were then extracted for each haploid bee from the *nearcticus*-Central population at these SNPs and scored according to parental allele state (allowing 10% missing data, thinned to one SNP per 100bp). This analysis is facilitated by the haploidy of all *nearcticus*-Central bees, which allows visualization of fully phased haplotypes across each scaffold. If recent hybridization had occurred, this would be apparent as large blocks of admixed parental sequence.

Supplementary files for bioinformatic analyses are available on Dryad ([doi.org/10.5061/dryad.7d7wm37r9](https://doi.org/10.5061/dryad.7d7wm37r9)), Sequencing data available for utilized genomic samples are available on NCBI BioProject PRJNA592825.

#### Genotyping for nuclear markers

Genomic data sampling includes only a single inferred *nearcticus* in sympatry with a single *bifarius* s.s. To examine for signs of genomic admixture in regions of sympatry with larger sample sizes, we examined variation in two nuclear markers

across 66 individuals representing the geographic range of the lineages of interest, including six *nearcticus* and seven *bifarius* s.s. specimens from three regions of sympatry (Book Cliffs, Uinta and Manti-La Sal mountain ranges in Utah), and two individuals of *vancouverensis* (Table S1). These markers were chosen as they have multiple synonymous SNPs (i.e. less likely to be under selective pressure than nonsynonymous ones) that were fixed between disjunct *nearcticus*-West and *bifarius* s.s. populations in a previous study (Lozier *et al.*, 2016a), and are thus informative for detecting allele sharing between sympatric individuals with minimal complications from incomplete lineage sorting. We designed primers for these markers that are complete matches to sequences of both forms by considering the alignment of SNPs for these populations against their respective homologues in *B. impatiens* (NCBI GenBank Assembly GCA\_000188095.3, BIMP\_2.1). We amplified 924 bp of the *serrate RNA effector* (BIMP21906, *Drosophila* ortholog *Ars2*), a gene involved in RNA transport and processing, using the designed primers SerF-a (5' CGAAAGCAGATCCTCGTAAGT 3') and SerR-ab-4 (5' GGCATTCGTCTTCGTTTGG 3'), and 610 bp of the *sodium/potassium-exchanging ATPase subunit alpha* (BIMP10181, *Drosophila* *Atpalpha*), a gene involved in salt ion homeostasis, using ATPF-b (5' TGCTGCAAA-CATGATGAAC 3') and ATPR-b-3 (5' ACCAGCAATC-CTTCCCATTAC 3'). Amplification of both loci were performed using the following cycle parameters: a first cycle of 30 s at 94°C, 40 s at 45°C, 1 min at 72°C, followed by 35 cycles of 30 s at 94°C, 40 s at 55°C, 1 min at 72°C, before final elongation of 10 min at 72°C. Previously identified fixed-divergence SNPs in these amplicons were compared among samples along with their mitochondrial haplotypes to assess for signs of introgression. Sequences are available on GenBank (Accession numbers MN781540-MN781579 for the ATPase; MN788377-MN788416 for the serrate RNA effector).

### Morphological analysis

We qualitatively examined barcoded specimens of both sexes covering a large part of the *B. bifarius* s.l. range (Alaska to Colorado) for morphological differentiation, focusing on cuticular characters (e.g. shape and puncturing of the clypeus, labrum, cheek, abdominal segments, ocellar area, corbiculae) that are generally considered as reliable characters for species-level discrimination in bumble bees (Williams *et al.*, 2010, 2014, 2019). For males, we examined the genitalia in more detail (shape and/or pile of the volsella, penis valve, gonostylus, gonocoxite and gonobase). As the shape of the medio-apical part of the eighth ventral plate of the males was argued to be distinct between *nearcticus* and *bifarius* s.s. by Stephen (1957), we more closely examined and imaged this sternite across specimens. For imaging, the 8<sup>th</sup> ventral plates were dissected from specimens relaxed in an ethanol:water dilution series. These were mounted in glycerol between two cover slips and imaged with an Olympus BX43 compound microscope with an attached Olympus DP73 digital camera. Image series were aligned and stacked using ZERENE STACKER (v1.04 Build T201404082055) and exposure was corrected in Adobe PHOTOSHOP CC 2019.

### Species distribution modelling

To examine whether the two lineages inferred with genetic data occupy distinct niche spaces, we estimated habitat suitability by species group using the maximum entropy approach applied in MAXENT v3.4.1 (Phillips *et al.*, 2004; Phillips & Dudík, 2008). This program is especially well-suited for presence-only datasets and can create accurate predictions from relatively small sample sizes (Phillips & Dudík, 2008). However, as MaxEnt is susceptible to overfitting and spatial autocorrelation, care should be taken to sample occurrence records evenly across space as well as to select appropriate model parameters. We combined specimen occurrence records confirmed as *nearcticus* or *bifarius* s.s. using *COI*, with additional localities of specimens determined to be *nearcticus* vs. *bifarius* s.s. using genetic data by Lozier *et al.* (2016a, 2016b). Occurrence records were distributed throughout the range extent and were limited to unique sites to minimize spatial bias prior to niche modelling (*bifarius* s.s.,  $n = 22$ ; *nearcticus*,  $n = 81$ ). Previous ecological niche analyses on *bifarius* s.s. determined that eight climatic variables (annual precipitation, maximum temperature of the warmest month, mean temperature of the wettest quarter, precipitation of the driest month, annual mean temperature, precipitation of the wettest month, mean temperature of the driest quarter and minimum temperature of the coldest month) aptly describe the climatic trends pertinent to montane bumble bee habitat suitability (Lozier *et al.*, 2013), thus we built our models using these variables. Contemporary climatic (averaged across the years 1970–2000) raster layers were downloaded at a resolution of 2.5 arc-minute from WorldClim v1.4 (Hijmans *et al.*, 2005), clipped to our study extent (-150, -103, 30, 65), and converted to an ASCII file in R/RASTER (Hijmans, 2018). Species-specific niche models were created using the default parameters applied in MAXENT v3.4.1 averaged across 15 cross-validated replicates. Model performance was assessed using the AUC statistic and variable permutation importance was determined using jack-knife analysis (Phillips *et al.*, 2004; Phillips & Dudík, 2008; Phillips *et al.*, 2017). The plot combining the predicted distribution of both *bifarius* s.s. and *nearcticus* was visualized in QGIS (Quantum GIS 2018), whereas the species-specific plots were visualized in R/RASTER (Hijmans, 2018) and R/GGPlot2 (Wickham, 2016) packages. In addition, we determined using the Student's *t*-test whether parameters differed between *bifarius* s.s. and *nearcticus*. We also ran *t*-tests on altitude for each variant for all specimens but also on Utah specimens alone, to determine whether *bifarius* s.s. occupies different altitude around contact zones.

## Results

### Mitochondrial phylogeny and haplotype network

The Bayesian inference conducted on the mitochondrial *COI* gene highlighted a species-level divergence between the taxa *bifarius* s.s. and *nearcticus* with strong support, as each comes out as a clade of lower sequence divergence (<2.0%, 0.5% on

average) subtended by long branches (Fig. 2A) with a ~6.9% pairwise *COI* sequence divergence between them. *bifarius* s.s. + *nearcticus* were resolved as sister lineages with *B. ternarius* as the closest relative. *Bombus ternarius* has less *COI*-divergence with *bifarius* s.s. (~3.0% divergence) than *bifarius* s.s. shares with *nearcticus* (6.9% divergence). No evidence for population structure was found within *bifarius* s.s., whereas some regional taxon clustering could be observed within *nearcticus*, although global population structure in the latter remained weak relative to species-level differences. The taxon *vancouverensis* was contained as a derived lineage within *nearcticus*. The three newly sampled *vancouverensis* specimens were a sister lineage to three British Columbia barcoded specimens from the same island chain, which are also likely *vancouverensis*, and these are derived from a clade that spans the Pacific coastal states and provinces. The PTP partition with the most support recognized seven candidate species (outgroup *B. melanopygus* not included in the analysis) as most likely (see the grey values accompanying the posterior probabilities; Fig. 2A), including all currently recognized species and separate species assignments for *nearcticus* and *bifarius* s.s., but not for *vancouverensis*.

The haplotype network analysis (Fig. 2B) shows that the two haplotypes for the *bifarius* lineage only occur in the Southern Rocky Mountains (eastern Utah and Colorado), and the 29 haplotypes for the *nearcticus* lineage occur west of this region, with haplotypes for the lineages only overlapping in a narrow contact zone (Fig. 2C). Although most satellite haplotypes diverged from the core haplotypes by a single base pair only, individuals from more distant sampling zones (e.g. Alaska) showed a stronger divergence from other relatives. Although weak population structure was highlighted by mapping *nearcticus* haplotypes (e.g. northern California/southern Oregon), specimens coming from close areas also can possess diverse mitochondrial haplotypes (e.g. northern Oregon, Utah).

### Genomic analysis

*Individual-level analysis of genomic relationships.* The PCA on the filtered individual-level SNP dataset of genomic samples exhibit clustering by population – *nearcticus*-West, *nearcticus*-Central, *vancouverensis* and *bifarius* s.s. – in the first two principal components, with *bifarius* s.s. distinguished from *nearcticus* + *vancouverensis* in the first principal component (15.13% of variation) and geographical separation of *nearcticus* + *vancouverensis* samples on the second (5.71% of variation) (Fig. 3B). This result is consistent with the phenogram (Fig. 3C), and with sNMF analysis results (Fig. 3D), where  $K = 2$  is the optimal number of population clusters (Figure S1) and *bifarius* s.s. is designated as a separate group from a combined *nearcticus*-West, *nearcticus*-Central and *vancouverensis* population (Fig. 3D). The *nearcticus* and *bifarius* s.s. samples from the same location in the Uinta mountains remained distinct to their respective populations across all analyses (Fig. 3, marked with a ‘U’). The *vancouverensis* specimen consistently was placed in the *nearcticus* clade across analyses, although with a slightly longer branch length in the phenogram and in

between western and eastern *nearcticus* clades along axis 2 in the PCA.

*Population-level divergence and admixture across the genome.* Differentiation and divergence across the genome were significantly higher between *bifarius* s.s. and both *nearcticus*-West (mean  $F_{ST} = 0.14$ ,  $d_{XY} = 0.46$ ) and *nearcticus*-Central (mean  $F_{ST} = 0.13$ ,  $d_{XY} = 0.46$ ) than for any intra-*nearcticus* window (mean  $F_{ST} = 0.01$ ,  $d_{XY} = 0.32$ ) (Fig. 4; Table S1). The differences between *bifarius* s.s. and either *nearcticus* lineage across the genome were highly correlated, consistent with strong *bifarius* s.s.–*nearcticus* differentiation and weak intra-*nearcticus* differentiation. Divergence ( $d_{XY}$ ) for the *nearcticus* population pair can be almost perfectly explained by mean  $\pi$  (simple regression slope = 0.98,  $R^2 = 0.96$ ), as expected if samples actually come from a single population and divergence simply reflects diversity. By contrast,  $d_{XY}$  in *bifarius* s.s.–*nearcticus* pairs greatly exceeded their mean  $\pi$  (Fig. 4). Alongside the overall signature of strong divergence between *bifarius* s.s. and *nearcticus*, there was some heterogeneity across the genome, particularly noticeable in blocks of sharply elevated  $F_{ST}$  and  $d_{XY}$  between *bifarius* s.s. and *nearcticus* (Fig. 4). Three blocks within scaffold JH157950 showed some notable intra-*nearcticus* elevation (Fig. 4, S2A). This region is also unusual in that  $d_{XY}$  exceeded mean  $\pi$  within *nearcticus* across much of the scaffold, especially in low diversity regions (Fig. 4). Notably, this scaffold corresponds to NT\_176739.1 from the BIMP 2.0 (Sadd *et al.*, 2015) RefSeq reference assembly, which was implicated in a previous transcriptome study as a potential target of selection in *nearcticus* (Pimsler *et al.*, 2017).

Consistent with the strong interlineage population structure, genome-wide evidence for widespread introgression between *bifarius* s.s. and *nearcticus* via geographically intermediate populations (UT+WY) was very low for the three population ABBA–BABA analysis. Confidence intervals from block-jack-knifing did not overlap zero ( $D = 0.005$ , 95% CI: 0.002–0.008;  $z$ -score = 3.1) so some weak historical admixture cannot be fully ruled out (Fig. S1; Table S1); however, average  $D$  across whole scaffolds ranged from –0.045 to 0.033, and none were significantly different from zero. The low  $f_{dM}$  value of 0.3% (0.1–0.5% 95% CI) likewise indicated little evidence for gene flow between lineages (Figure S1A). There is some evidence for more restricted introgression at certain portions of the genome that might explain the subtle excess of ABBA over BABA sites (Fig. 4). For example, one window in JH157950 (275–375kb), discussed above, reaches  $D = 0.43$  with an  $f_{dM}$  of 15.5%, the largest in the dataset, indicating an excess of shared polymorphism between *bifarius* s.s. and *nearcticus*-Central in this region (Figure S2A). However, this window contains Xanthine dehydrogenase/oxidase-like, a selection target previously identified from RNA-Seq SNPs (Pimsler *et al.*, 2017). Like the full three-population comparison, the model involving specification of a single *nearcticus* bee collected from a site of geographic overlap with *bifarius* s.s. in the Uinta mountains in UT also showed  $D$  and  $f_{dM}$  values surrounding zero (Figure

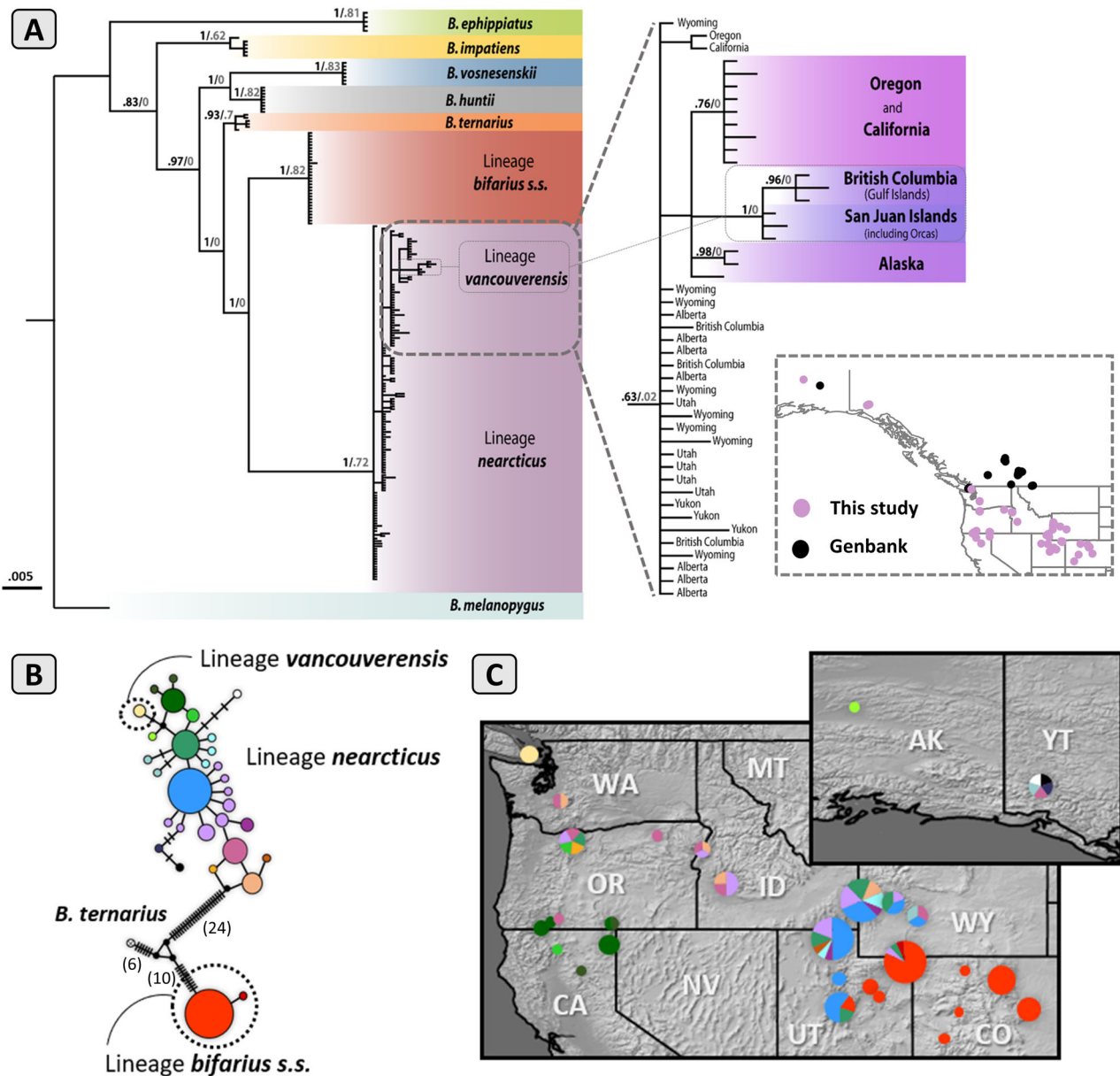


**Fig. 2.** Relationships of *Bombus bifarius* s.l. specimens inferred with cytochrome oxidase I (*COI*). (A) Bayesian tree of *B. bifarius* s.l. and close relatives based on the barcode fragment of the *COI*. Clade support values are Bayesian posterior probabilities (black) and PTP values in support of all daughter alleles belonging to a single species (grey). The right zoomed-in part of the figure highlights some population structure within the specimens of *vancouverensis*. The map shows the sampling locations of the specimens of *B. bifarius* s.l. used in the phylogenetic analysis with the original sampling of the study displayed in purple and the previously published sequences in black. (B) Haplotype network for the newly sequenced individuals, highlighting the connections between the haplotypes shown on the map (right). To avoid colour overloading, very closely related haplotypes (i.e. within 1 bp from a main core haplotype) share the same colour. (C) Visualization of the major haplotypes from the same sampling, mapped at their respective geographical locations. The sizes of the circles and pie charts are proportional to the number of haplotypes that they contain. [Colour figure can be viewed at [wileyonlinelibrary.com](http://wileyonlinelibrary.com)].



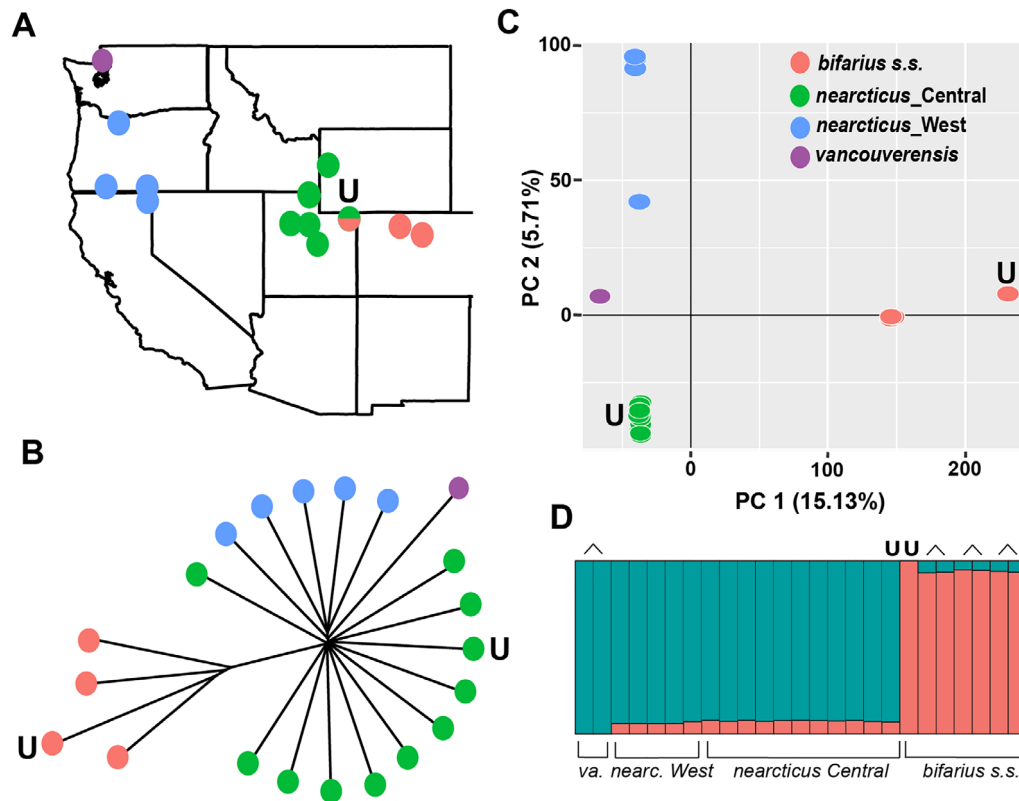


**Fig. 3.** Population structure inferred from whole-genome sequence data: (A) A map of sampled specimens, coloured to match respective clades in (B)–(D). (B) Principal component analysis (PCA) of the whole-genome single nucleotide polymorphism (SNP) data, showing the separation of *bifarius s.s.* from the *nearcticus* and *vancouverensis* populations. (C) Neighbour-joining unrooted phylogeny of SNP data. (D) sNMF analysis results for  $K = 2$ , with colours reflecting different population assignment. Carets (^) above the plots indicate differently phased samples from the same diploid individual. ‘U’'s represent two specimens obtained from the same locality and collecting event in the Uinta Mountains for (B)–(D). [Colour figure can be viewed at [wileyonlinelibrary.com](http://wileyonlinelibrary.com)].

S2B). Overall, such weak evidence for introgression should be considered with caution, with most of the genome suggesting a lack of ongoing gene flow between *bifarius s.s.* and *nearcticus* even in sites of sympatry.

Ancestry painting reveals that of the 5160 fixed divergent SNPs between the more distant *bifarius s.s.* and *nearcticus*-West lineages, 9–10% of each *nearcticus*-Central genome represented the *bifarius s.s.* allele (Figure S2C). However, these regions were haphazardly scattered across the genome, and there were no blocks of *bifarius s.s.* ancestry, so it is unlikely that any of these genomes are produced by recent introgression from *bifarius s.s.* Much of the shared variation can thus likely be explained by incomplete lineage sorting, as suggested by ABBA–BABA analysis. We repeated the ancestry analysis by specifying five haploid *nearcticus*-Central populations (to hold sample size equivalent to *nearcticus*-West) and examined SNPs with fixed alternative states between *bifarius s.s.* and *nearcticus*-Central, using *nearcticus*-West samples instead as the putative hybrids. Under a pure divergence history with incomplete lineage sorting, the same fraction of SNPs should show ancestry with *bifarius s.s.* in this test dataset as in the previous dataset. However, we saw a slightly smaller proportion of SNPs with

*bifarius s.s.* ancestry in *nearcticus*-West (Wilcoxon rank sum test:  $P < 0.001$ ) compared to *nearcticus*-Central, which is consistent with the small but significant  $D > 0$ .

#### Nuclear genotyping

Clustering based on the genotyping across seven SNPs of both nuclear markers matched the clustering based on the mitochondrial *COI* for all individuals, including all specimens coming from sympatric areas (Fig. 5; Table S2). A single SNP among four for the ATPase was heterozygous for a few of the *B. bifarius s.s.* Although this could be considered as a sign of gene flow, given the alleles of linked SNPs, it is likely indicative of a lack of complete historic lineage sorting at this particular SNP. The *vancouverensis* bees do not differ from the other *nearcticus* at either nuclear locus.

#### Morphological analyses

Using qualitative approaches, no obvious external morphological character could be found to reliably discriminate between

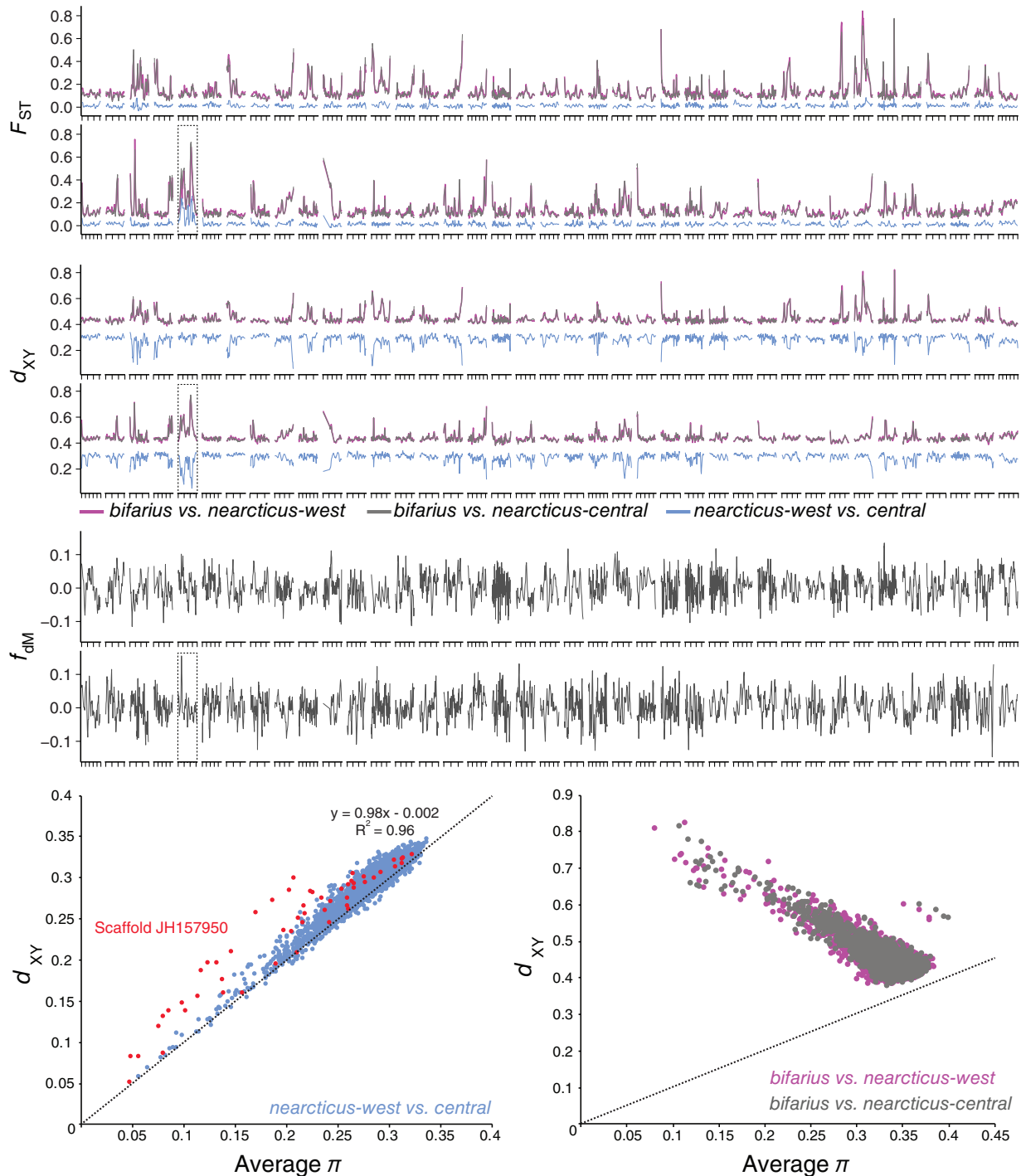


**Fig. 4.** Genome-wide estimates of  $F_{ST}$ , absolute divergence  $d_{XY}$ , and the introgression statistics  $f_{dM}$  (ABBA–BABA topology: P1 = *nearcticus*-West; P2 = *nearcticus*-Central; P3 = *bifarius* s.s.) for 100-kb sliding windows (25 kb slide/step) with at least 100 single nucleotide polymorphisms (SNPs) in the three *Bombus bifarius* s.l. lineage comparisons. Data are shown for 78 *B. impatiens* scaffolds with length >1 Mb, where x-axis tick markers each represent 500 kb. In the  $F_{ST}$  and  $d_{XY}$  plots, both *bifarius* vs. *nearcticus* plots overlap nearly perfectly so they are largely indistinguishable. Scaffold JH157950 is demarcated with a dotted rectangle. The bottom plots show the relationship between absolute divergence  $d_{XY}$  between population pairs and mean nucleotide diversity ( $\pi$ ) for the pair being considered (left = within-*nearcticus* divergence, right = *bifarius* s.s. vs. *nearcticus* divergence). Within *nearcticus* interpopulation divergence is essentially equivalent to intrapopulation diversity for each region of the genome (except for regions in scaffold JH157950 highlighted in red), whereas divergence greatly exceeds mean diversity for *bifarius* s.s. vs. *nearcticus* comparisons. The dashed line shows equal diversity-divergence in each panel. [Colour figure can be viewed at [wileyonlinelibrary.com](http://wileyonlinelibrary.com)].

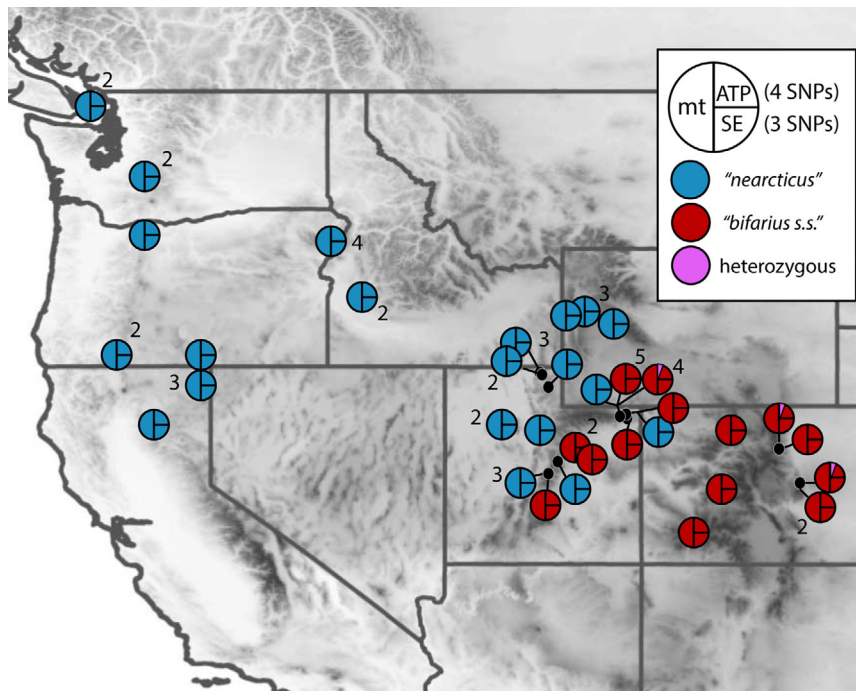


**Fig. 5.** Distribution and allelic designation of individuals sampled for nuclear genotyping, showing the close association between mitochondrial and nuclear haplotypes. Pie charts represent haplotype combinations at a locality; each one shows whether the specimen's haplotype was designated as being allied to the *Bombus nearcticus* vs. *bifarius s.s.* lineage (Fig. 1) using mitochondrial data on the left side. In comparison to mitochondrial data, on the right side of the pie, the four single nucleotide polymorphisms (SNPs) of the ATPase (ATP) and the three SNPs of the Serrate Effector (SE) are designated, using different colours for whether the allelic variant matches the fixed alleles for western *nearcticus* (blue) vs. *bifarius s.s.* (red) from a previous study (Lozier *et al.*, 2016a). A few individuals had heterozygosity at a single ATPase SNP, indicated in pink. Numbers next to pie charts indicate the number of individuals with that haplotype combination in localities where more than a single individual were sampled. Localities were combined if sites were very close with the exception of the hybrid zone in Utah, where all localities are indicated separately to show allelic patterns of individuals in sympatry. Three pie charts that also were all blue ('*nearcticus*') from Alaska and Yukon are not shown. An altitude layer is overlaid in the background with higher altitudes shaded darker. Data are further represented in Table S2 and specimen details in Appendix S1. [Colour figure can be viewed at [wileyonlinelibrary.com](http://wileyonlinelibrary.com)].

the females of *nearcticus* and *bifarius s.s.* For males, we found that the shape of the medio-apical ridge of the eighth ventral plate, previously reported as distinct between lineages, showed high variability and thus is not a reliable interspecific discriminant character (Figure S3). Thus, these two lineages can only be discriminated outside of DNA sequences based on coloration, in part, combined with information on geographical range (see below).

#### Species distribution prediction

Species distribution models predict that *bifarius s.s.* (AUC = 0.981, SD = 0.014) and *nearcticus* (AUC = 0.884, SD = 0.057) occupy somewhat different niche spaces, with *bifarius s.s.* occupying a narrower spatial projection of the environmental niche. Despite limited realized overlap in geographical ranges, predicted niches overlap in distribution throughout portions of the Rocky Mountains (Fig. 6). For example, the niche model predicts that *bifarius s.s.* is distributed at mainly high elevation locales throughout the eastern portions of the Rocky Mountain chain, whereas available specimen

data suggest that it is largely confined to the Southern Rocky Mountains. When comparing values for the niche variables between each form, only four variables differed significantly (Table S3). The taxon *nearcticus* tends to occupy wetter areas on average ( $P = 0.021$ ), but the range of precipitation fully spans that of *bifarius s.s.* (Figure S4). The *nearcticus* clade also varies in temperature in the driest quarter ( $P = 0.0022$ ) and mean temperatures of the wettest quarter ( $P = 0.041$ ), likely because the wet season is different between the Pacific west and the Rocky Mountains. Furthermore, *bifarius s.s.* occupies higher elevations than *nearcticus* ( $P < 0.001$ ; Figure S3). In Utah, where zones of sympatry occur, *bifarius s.s.* also differs in altitude ( $P = 0.033$ ) occurring in the highest elevation zones of *nearcticus*.

## Discussion

#### Species-level differentiation

We utilized an integrative approach gathering mitochondrial *COI* barcode data, targeted nuclear gene sequencing and

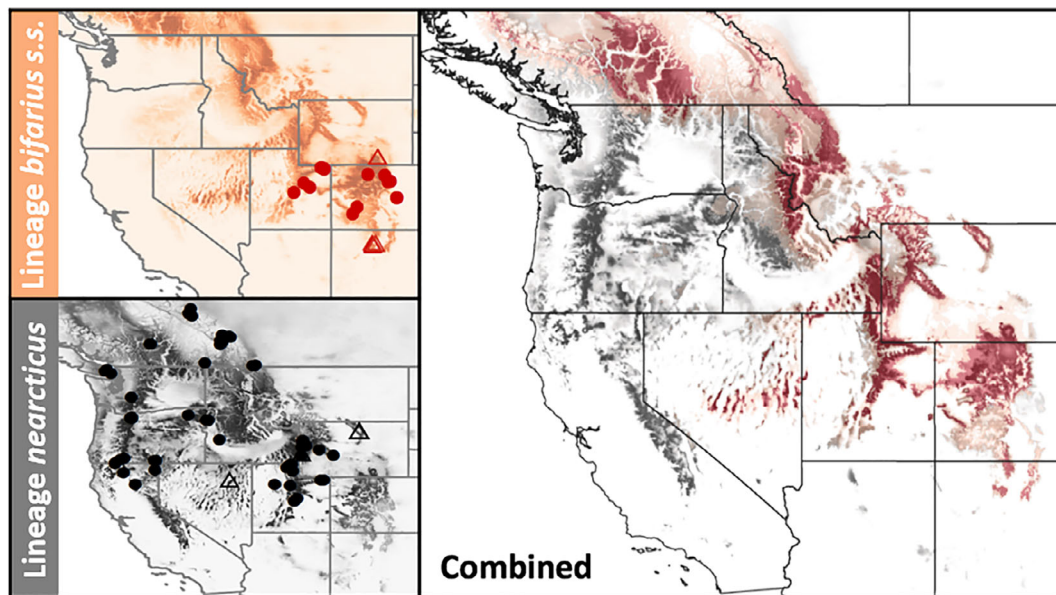


**Fig. 6.** MAXENT predictions based on unique occurrence data for the lineages *Bombus bifarius* s.s. ( $n = 22$ ) and *nearcticus* ( $n = 81$ ), using only specimens identified based on nuclear and mitochondrial sequence data. Left: *nearcticus* and *bifarius* s.s. niche models. Triangles represent localities from Lozier *et al.* (2013, 2016a), and circles represent individuals identified herein with barcode data. Darker colours are more suitable niches. Right: Combined model for both lineages *nearcticus* (black) and *bifarius* s.s. (red). [Colour figure can be viewed at [wileyonlinelibrary.com](http://wileyonlinelibrary.com)].

whole-genome sequencing to achieve a robust understanding of patterns of divergence and gene flow in *B. bifarius* s.l. Our high spatial resolution analysis of *COI* across the geographical range of this species complex revealed strongly supported species-level differentiation that roughly corresponds to the historically recognized lineages *bifarius* s.s. and *nearcticus*. These two lineages exhibit high interlineage divergence (6.9%) and low intralocus divergence, a pattern of phylogenetic differentiation that is typically indicative of species-level differentiation (Hebert *et al.*, 2003). The divergence between *bifarius* s.s. and *nearcticus* is concordant for *COI* and a set of diagnostic nuclear SNPs, further supporting a lack of ongoing gene flow between the two lineages. Finally, we find consistent evidence for the two major lineages from whole-genome analyses of differentiation and divergence. Individuals belonging to these two respective lineages are largely separated geographically, with *nearcticus* in the western part of the range and *bifarius* s.s. confined to the Southern Rocky Mountains surrounding the Colorado Plateau. This analysis revealed three fairly narrow regions of sympatry in the Uinta, Book Cliffs and Manti-La Sal mountain chains of Utah (Fig. 5; Table S2). Despite the opportunity for allele sharing in these regions, no recent gene flow was inferred from the genomes of individuals in sympatry or from targeted nuclear markers with increased taxon sampling at these zones.

Analyses utilizing whole-genome sequencing data suggest some possibility of weak introgression between *bifarius* s.s. and *nearcticus* via geographically proximate *nearcticus*-Central populations (Figure S1). However, we see very little evidence for large blocks of shared ancestry in genome scans (Fig. 4) or ancestry painting (Figure S1); given the perfect phasing of haploid *nearcticus* samples, introgressed haplotypes should be

readily apparent if recent ongoing gene flow was contributing to shared variation. Thus, it seems more likely that any admixture is infrequent or has occurred well into the past. Furthermore, inferring gene flow from ABBA–BABA statistics relies on assumptions of the underlying demographic model, and similar values can be produced under both introgression and ancestral population structure (Martin *et al.*, 2015). Finally, we suspect that some of the positive  $D$  and  $f_{DM}$  signatures may result from selection. One scaffold, JH157950 (GenBank assembly, BIMP 2.1), showed notable intra-*nearcticus* differentiation that exceeded other regions of the genome, and was the only scaffold where  $F_{ST}$  within *nearcticus* exceeded the lowest observed  $F_{ST}$  between *bifarius* and *nearcticus*. The sharp discrepancy between  $F_{ST}$  and  $d_{XY}$  in this interval (Fig. 4; Figure S1) potentially suggests the action of a selective sweep in the ancestral population (Cruickshank & Hahn, 2014).

Altogether, our different types of genetic data, combining high-resolution spatial sampling at small numbers of mitochondrial and nuclear markers with high-resolution genomic sampling of spatially representative populations, reject the presence of common recent gene flow between the two taxa, hereby leading us to designate these lineages as separate species.

#### Population-level distinctions

Within-lineage divergence is low, although the more widespread *nearcticus* demonstrates some clustering of eastern (intermediate or mostly red coloured) individuals from western (mostly black forms) using genomic data. Lozier *et al.* (2016a) observed similar population structure among eastern

and western populations from transcriptome and reduced representation (ddRAD) sequencing. The *COI* data showed minor geographical structure in *nearcticus* in more peripheral populations, but haplotype variants as a whole tend to be broadly admixed across much of the western United States. In the whole-genome data,  $F_{ST}$  was near zero and  $d_{XY}$  was not substantially different from  $\pi$  for the *nearcticus* populations, as expected if samples are drawn from a single population. These data are in line with previous genetic data which suggest that landscape heterogeneity likely restricts gene flow leading to genetic differentiation following an isolation-by-distance model shaped by the arrangement of suitable habitat (Lozier *et al.*, 2013; Jackson *et al.*, 2018).

The lineage *vancouverensis*, once recognized as a separate species, is here supported in all sequencing results as a derived clade within *nearcticus* that is closely related to other specimens from the Pacific coastal states and provinces. The branch length of this clade is a bit higher in genomic analyses and there is some *COI* divergence (0.6%) from sister clades of *nearcticus*, an expected pattern given that it is an island population with restrictions on gene flow. In the light of these findings, and given their distinct colour pattern from neighbouring mainland populations, restricted distribution and previous population genetic results indicating high levels of differentiation for the San Juan Island populations (Lozier *et al.*, 2011), we consider the latter specimens as belonging to a subspecies that is distinct from the one occurring on the continent, but not sufficiently distinct to warrant species-level separation from the remaining *nearcticus*.

#### Crypticism and mimicry

We did not find any reliable cuticular characters to diagnose individuals belonging to either species. Stephen (1957) previously considered the terminal male sternite to be different between the two, but we found this character to be highly variable and also not diagnostic. In the absence of clearly diagnostic external characters, and until more detailed quantitative analyses of internal and external characters are performed, these can be considered a case of cryptic speciation. The most reliable way found to diagnose them aside from genetic sequencing, is through assessing their coloration and locality. However, colour also can fail as a diagnostic character in regions of sympatry where *nearcticus* individuals exhibit colour most similar to *bifarius* s.s. (Figure S6). This lack of discriminant cuticular characters is not surprising within the subgenus *Pyrobombus*, for which many identification keys rely on pile colour to allow species-level identification (Stephen, 1957; Thorp *et al.*, 1983; Koch *et al.*, 2012; Williams *et al.*, 2014).

The presence of numerous intermediate colour forms in the *B. bifarius* s.l. species complex between the westernmost Pacific region (black-banded) and the southeastern specimens (red-banded) previously led to the conclusion that continuous gene flow was occurring across this lineage, thus leading to synonymization of previously described species (Stephen, 1957; Williams *et al.*, 2014). In this case, colour traits have led

taxonomists astray. Coloration has often led to false inferences of species delimitation in bumble bees. Some species historically described by discrete colour differences have been revealed to be conspecific, as discrete morphologies can be generated from diallelic Mendelian traits (Owen & Plowright, 1980; Rasmont *et al.*, 2005; De Meulemeester *et al.*, 2011). Failure to fully sort ancestral colour polymorphisms by species also has led to false inferences of species boundaries (Hines, 2008; Carolan *et al.*, 2012; Koch *et al.*, 2018; Williams *et al.*, 2019). In this instance, *bifarius* s.s. is a monomorphic red-banded bee species and *nearcticus* is a polymorphic species that follows a continuum of variation from black to red from west to east (excepting island populations). At the root of this confusion are issues with using colour traits influenced by Müllerian mimicry (Hines & Williams, 2012). North American mimicry complexes involve darker colour forms in the Pacific coastal regions and red colour forms in the Rocky Mountains. Higher fidelity patterns can be found in the far west and east, respectively, of these ranges, with lower fidelity patterns in between (Ezray *et al.*, 2019). Thus, *bifarius* s.s. is seemingly converging on the abundant high-fidelity pattern in the southern Rocky Mountains, whereas *nearcticus* is converging on the most abundant patterns in its respective regions, showing fidelity matching the colour continuum that occurs across its range.

Convergence upon the high-fidelity Rocky Mountain pattern in the East could alone explain colour similarities in areas of sympatry. However, it also is possible that similarities in coloration between eastern *nearcticus* and *bifarius* s.s. could result from historical patterns of allele sorting and/or gene flow. The examination of admixture across the genome revealed a single genomic interval with high differentiation between the western black and eastern mostly-red *nearcticus*, a region that also has a relatively high percentage of ABBA–BABA allele sharing between *bifarius* s.s. and mostly red ‘central’ *nearcticus* populations. This interval falls in the same contig as the one inferred to potentially harbour a gene for coloration in this species inferred from transcriptome sequencing (Xanthine dehydrogenase/oxidase-like; Pimslers *et al.*, 2017). Alleles for red coloration may have undergone adaptive introgression from *bifarius* s.s. to *nearcticus* to generate its red mimetic phenotype, similar to what was observed in *Heliconius* mimicry (Pardo-Diaz *et al.*, 2012), or could result from sorting of colour variation from a polymorphic ancestor. Alternatively, black-associated alleles may be derived from ancestral red-associated alleles within *nearcticus*, with polymorphism in *nearcticus* maintained through selection, thus driving low effective population sizes and corresponding genetic diversity in this interval. Haplotypes of the Xanthine dehydrogenase/oxidase-like gene show unusual relationships compared to the genome as a whole that is more consistent with ancestral polymorphism than recent introgression (Pimslers *et al.*, 2017), supporting the selective sweep hypothesis. Indeed, the entire JH157950 contig shows somewhat unusual patterns in *nearcticus*, suggesting that there could be some interesting genomic architecture relating to phenotypic variation in the region. By resolving species status and taxonomy in this study, we now open the door for a more informed investigation into

evolutionary forces that may drive polymorphism and mimicry in this complex and a closer examination of the genome regions that may be driving speciation.

#### Niche occupation

The narrow region of sympatry observed in these two species suggests that some factor must maintain these lineages separate from one another and thus be important for their speciation. For our two taxa of interest, species distribution modelling previously has been found to effectively explain genetic differentiation at the population level (Lozier *et al.*, 2013; Jackson *et al.*, 2018). Species distribution modelling performed on *bifarius* s.s. and *nearcticus* separately, as defined by barcode sequences, inferred that *bifarius* s.s. occurs in drier areas and at higher elevations than *nearcticus*. Although altitude could ultimately be a primary factor differentiating them, this variable may be influenced by its more southern geographical location (e.g. Williams *et al.*, 2016) and the effects of drier climate on altitudinal distribution. With the variables tested, these species distribution models also predict that the species should overlap. Models thus raise the question regarding factors that prevent more substantial co-occurrence of these species. Given that occasional darker forms have been recorded in Colorado and some unusually red forms have occurred further west in museum specimen data (Fig. 1), this may suggest that the region of overlap may be broader than identified with our sampling. Our improved taxonomy, together with more extensive geographic sampling, will be of value for resolving discrepancies between the realized and predicted ranges of these species and identifying the factors that have contributed to their spatially limited coexistence and potentially to the maintenance of their genetic isolation.

#### Revised species status

Given the strong congruence of our results, also supported by previous analyses at the RNA (RNA-Seq), DNA (ddRAD-Seq) and phenotypical levels (Lozier *et al.*, 2016a), we resurrect both lineages *bifarius* s.s. and *nearcticus* to species status. *Bombus bifarius* Cresson was originally described from a type series including males and females as being a bee with red in T2 and T3 except for a black anteromedial v-shaped notch in T2; however, individuals from regions where we only found darker forms of *nearcticus*, such as in the region around British Columbia, are included in the description. We have observed the lectotype of *B. bifarius* Cresson at The Academy of Natural Science of Drexel University (Philadelphia, U.S.A.), a queen that was labelled and formally designated as the lectotype by Cresson (Cresson, 1916) after the original description (Cresson, 1878). This lectotype (Figure S5A,B), carrying the labels (i) white, printed 'Col.' and (ii) red, printed 'LECTOTYPE' / handwritten '2628' corresponds to the typical red-banded individuals of the *bifarius* s.s. from Colorado sequenced here. Therefore, this gives the eastern lineage the name *B. bifarius* Cresson.

In the same paper, Cresson (1878) also described the species *B. vancouverensis* Cresson from a type series including several males and a female available in the same collection (Figure S5C,D). Cresson (1916) had designated a male from Vancouver Island, British Columbia as the lectotype, carrying the labels: (1) white, printed 'Van.' and (2) red, printed 'LECTOTYPE' / handwritten '2644'. Although the colour has faded on many of these specimens, including the lectotype, the morphology and colour pattern match that corresponding to the lineage herein referred as *vancouverensis* from the San Juan Islands, with a paler yellow on the thorax evident in some of the specimens, and mostly red on T2 + T3. Finally, we requested from the Naturhistorisches Museum Wien (Vienna, Austria) individuals from the *nearcticus* type-series. Only one individual, identified by Handlirsch himself, phenotypically corresponding to his original description and agreeing with the collection data referred to by Handlirsch (1888), was located (Figure S5E,F). To reduce uncertainty in the identity and application of the name, we assigned a lectotype status to this female individual carrying the labels: (i) white, printed 'Brit. Col'; (ii) white, handwritten 'nearcticus' / printed 'det. Handlirsch'; (iii) white, printed 'Bombus' / handwritten 'bifarius / var. nearcticus' / printed 'det. Babiyy'; (iv) white, printed 'Pyrobombus / b. nearcticus (Handl.) / Det. Milliron 1962 [female]; (v) white, printed 'NHM'; (vii) white, printed 'NHMW'; (vii) red, handwritten 'Rasmont det. 2019' / printed 'LECTOTYPE' [female] / handwritten 'Bombus nearcticus / Handlirsch'; (viii) printed 'det. P. Rasmont 2019 / Bombus (Pyrobombus) / vancouverensis nearcticus / Handlirsch'. The colour pattern of the specimen (with the T2–3 fully covered with black pile) also distinctly corresponds to most western specimens herein referred to as *nearcticus*. As we find the lineage *vancouverensis* conspecific with *nearcticus* based on sequencing data, the name *B. vancouverensis* Cresson consequently holds precedent by 10 years over *nearcticus* Handlirsch. Therefore, we recognize two distinct species within the *B. bifarius* s.l.: *B. bifarius* Cresson and *B. vancouverensis* Cresson. In addition, because of the previously mentioned divergence of the island populations near Vancouver with the continental *vancouverensis*, we consider two subspecies within *B. vancouverensis*: *B. vancouverensis vancouverensis* **comb.n.** (occurring on Vancouver Island and the surrounding islands of the Salish Sea, phenotypically similar to the types described by Cresson in 1878) and *B. vancouverensis nearcticus* **comb.n.** (occurring in the western part of the continent, phenotypically similar to the specimens described by Handlirsch in 1888).

These species are best diagnosed given their barcode sequences (Appendix S1; e.g. *B. bifarius* NCBI MN781432, *B. vancouverensis nearcticus* NCBI MN781514). They also can be diagnosed to some degree by colour (Fig. 1) and geographical range (Fig. 6). *Bombus bifarius* in all cases examined was fully red in females in T2/T3 aside from an anteromedial V-shaped black region in T2 for some females and is typically fully red in males. In *B. vancouverensis nearcticus* **comb.n.** females typically have all black in T2 and T3 in western Oregon and Washington and throughout California. Some red occurs on segments T2 and T3 east of the Pacific coastal mountains starting in the westernmost Rocky Mountains and increasing in amount

eastward (Fig. 1), but the amount of black is nearly always more than *B. bifarius*. Females in regions of sympatry tend to exhibit <80% red in T2+T3 in *B. vancouverensis nearcticus comb.n.*, exhibiting a more pronounced black 'V' extending from the anteromedial border of T2, as opposed to >80% red and a smaller 'V' in *B. bifarius* (Figure S6; cf. Fig. 1 top vs. middle right bee). Males in the region of sympatry are often fully red for both forms but can exhibit some black in *B. vancouverensis nearcticus comb.n.* Finally, *B. vancouverensis vancouverensis comb.n.* females present a distinctly paler thoracic coloration (cream-white, by contrast with the yellowish coloration of *bifarius* and *vancouverensis nearcticus comb.n.*) with a majority red coloration in T2+T3, involving black in the anterior portion of T2 and extending posteriorly into T3 in a V-shaped notch. The distinction between cream and yellow colours is reduced in males, which tend to be mostly red in T2+T3. Males and to a lesser extent, females, of *B. bifarius*, *B. vancouverensis nearcticus*, and *B. vancouverensis vancouverensis* can have a yellow arch in place of the V-shaped notch in T2. The amount of red in *B. vancouverensis vancouverensis* is considerably greater than neighbouring mainland population of *B. vancouverensis nearcticus comb.n.*, which are almost exclusively black.

#### *Species concepts and the conservation of cryptic diversity*

This study highlights how multi-trait approaches including powerful genomic tools and ecological modelling constitute a robust framework to uncover and explain patterns of population structure and inconspicuous speciation in cryptic organisms. Lineages such as *B. bifarius/B. vancouverensis* that lack gene flow even in sympatry, and thus adhere to most species concepts, may not yet have evolved sufficient fixed morphological variation. Criteria that disallow morphologically cryptic lineages may thus be prone to false negatives.

Taxonomic incompleteness constitutes a fundamental obstacle to invertebrate conservation worldwide, limiting understanding of species distribution and ecology and the ability to effectively conserve taxa (Cardoso *et al.*, 2011). Underestimations of cryptic biodiversity can now be unveiled by the use of integrative molecular taxonomic approaches (e.g. Fujita *et al.*, 2012; Fontaneto *et al.*, 2015) such as those used herein. Bumble bees are highly valuable pollinators in natural and agricultural ecosystems (Kremen *et al.*, 2002; Velthuis & Van Doorn, 2006), as well as an emerging model system for evolutionary genetics (Tian *et al.*, 2019), and thus have a robust history of taxonomic and phylogenetic revision. However, as this study reveals, there is still a need to improve our understanding of species delimitation in these bees, even in some of the most common species. The formerly recognized *Bombus bifarius* s.l. was regarded as one the most common and widespread species in North America. This study highlights a need to reassess the relative abundance and species status of the lineage (*B. bifarius* vs. *B. vancouverensis*) as newly circumscribed. Eco-climatic perturbations of confined niches including the high mountains involved in these species, are likely to have a substantial impact on bumble bee diversity in the future decades (Kerr *et al.*, 2015;

Rasmont *et al.*, 2015; Jackson *et al.*, 2018) which makes it ever more imperative to adequately recognize these species.

#### Supporting Information

Additional supporting information may be found online in the Supporting Information section at the end of the article.

**Appendix S1.** Specimen information including locality, haplotype from COI data, identification from nuclear and mitochondrial (mt) data, and accession number.

**Table S1.** Population genetics statistics for three population whole-genome sequencing data.

**Table S2.** Nucleotides obtained from ATPase and Serrate Effector genes compared to mitochondrial haplotypes.

**Table S3.** Contribution of the bioclimatic variables to the distribution models of *bifarius* s.s. and *nearcticus*.

**Figure S1.** Optimal numbers of populations for the sNMF analysis inferred from minimal cross-entropy.

**Figure S2.** Tests of admixture between sampled genomic populations in Figure 4: (A) A detailed depiction of scaffold JH157950 (highlighted with box in above plots). (B) Two introgression scenarios tested with the ABBA-BABA approach ( $D$  and  $f_{DM}$  statistics). (C) Ancestry painting analysis of fixed divergent SNPs between two specified 'parental' lineages (*bifarius* s.s. = black and *nearcticus*-West = grey) and the putative 'hybrid' (*nearcticus*-Central).

**Figure S3.** Morphological variation in the medio-apical ridge of the 8<sup>th</sup> ventral plate from randomly selected individuals.

**Figure S4.** The lineages *bifarius* s.s. and *nearcticus* yielded significant differences in the leading explanatory variable, annual precipitation (left). Altitude also significantly differs both overall and in Utah, where zones of sympatry are found (right).

**Figure S5.** Type specimens examined: (A,B) Lectotype of *Bombus bifarius* Cresson from *The Academy of Natural Science of Drexel University* (Philadelphia, U.S.A.) (Photos L. Tian). (C,D) Lectotype of *Bombus vancouverensis* Cresson from *The Academy of Natural Science of Drexel University* (Philadelphia, U.S.A.), revised here as *Bombus vancouverensis vancouverensis comb.n.* (Photos L. Tian). (E,F) Lectotype of *Bombus nearcticus* Handlirsch from the *Naturhistorisches Museum Wien* (Vienna, Austria), revised here as *Bombus vancouverensis nearcticus comb.n.* (Photos P. Rasmont).

**Figure S6.** The percent red (as opposed to black) coloration in metasomal tergites 2 and 3 combined across all specimens sampled from the three regions of sympatry (Manti-La

Sal site, Uinta Mountain sites, and the Western Book Cliff site).

## Acknowledgements

We would like to thank Baptiste Martinet for providing specimens from Alaska and Canada, Seth Davis for providing specimens from Colorado, Elyse McCormick for technical support during laboratory work, and Andy Deans for the use of microscope facilities. We also thank Paul H. Williams and an anonymous reviewer for their constructive comments on the manuscript. Funds for this research were provided by National Science Foundation grants DEB-1457645 to JDL, NSF CAREER DEB-1453473 to HHM, and F.R.S.-FNRS (Fonds de la recherche scientifique) in support of GG. The authors declare that they have no conflicts of interest.

## References

- Andrews, S. (2010) *FastQC: a quality control tool for high throughput sequence data* [WWW document]. URL <http://www.bioinformatics.babraham.ac.uk/projects/fastqc> [accessed in 2016]
- Bertsch, A. (2009) Barcoding cryptic bumblebee taxa: *B. lucorum*, *B. cryptarum* and *B. magnus*, a case study. *Beitraege zur Entomologie*, **59**, 287–310.
- Bickford, D., Lohman, D.J., Sodhi, N.S. et al. (2007) Cryptic species as a window on diversity and conservation. *Trends in Ecology and Evolution*, **22**, 148–155.
- Bolger, A.M., Lohse, M. & Usadel, B. (2014) Trimmomatic: a flexible trimmer for Illumina sequence data. *Bioinformatics*, **30**, 2114–2120.
- Bradbury, P.J., Zhang, Z., Kroon, D.E. et al. (2007) TASSEL: software for association mapping of complex traits in diverse samples. *Bioinformatics*, **23**, 2633–2635.
- Browning, S.R. & Browning, B.L. (2007) Rapid and accurate haplotype phasing and missing-data inference for whole-genome association studies by use of localized haplotype clustering. *The American Journal of Human Genetics*, **81**, 1084–1097.
- Cameron, S.A., Hines, H.M. & Williams, P.H. (2007) A comprehensive phylogeny of the bumble bees (*Bombus*). *Biological Journal of the Linnean Society*, **91**, 161–188.
- Cameron, S.A., Lozier, J.D., Strange, J.P. et al. (2011) Patterns of widespread decline in North American bumble bees. *Proceedings of the National Academy of Sciences USA*, **108**, 662–667.
- Cardoso, P., Erwin, T.L., Borges, P.A.V. & New, T.R. (2011) The seven impediments in invertebrate conservation and how to overcome them. *Biological Conservation*, **144**, 2647–2655.
- Carolan, J.C., Murray, T.E., Fitzpatrick, Ú. et al. (2012) Colour patterns do not diagnose species: quantitative evaluation of a DNA barcoded cryptic bumble bee complex. *PLoS ONE*, **7**, e29251.
- Corbet, S.A., Williams, I.H. & Osborne, J.L. (1991) Bees and the pollination of crops and flowers in the European Community. *Bee World*, **72**, 47–59.
- Cresson, E.T. (1878) Descriptions of new species of North American bees. *Proceedings of the Academy of Natural Sciences of Philadelphia*, **30**, 181–221.
- Cresson, E.T. (1916) *The Cresson types of Hymenoptera*. Memoirs of the American Entomological Society 1. American Entomological Society, Lanham, MD
- Cruikshank, T.E. & Hahn, M.W. (2014) Reanalysis suggests that genomic islands of speciation are due to reduced diversity, not reduced gene flow. *Molecular Ecology*, **23**, 3133–3157. <https://doi.org/10.1111/mec.12796>.
- De Meulemeester, T., Aytekin, A.M., Cameron, S. & Rasmont, P. (2011) Nest architecture and species status of the bumble bee *Bombus (Mendacibombus) shaposhnikovi* (Hymenoptera: Apidae: Bombini). *Apidologie*, **42**, 301–306.
- De Queiroz, K. (2007) Species concepts and species delimitation. *Systematic Biology*, **56**, 879–886.
- DePristo, M.A., Banks, E., Poplin, R. et al. (2011) A framework for variation discovery and genotyping using next-generation DNA sequencing data. *Nature Genetics*, **43**, 491–498.
- Der Sarkissian, C., Ermini, L., Schubert, M. et al. (2015) Evolutionary genomics and conservation of the endangered Przewalski's horse. *Current Biology*, **25**, 2577–2583.
- Duennes, M.A., Lozier, J.D., Hines, H.M. & Cameron, S.A. (2012) Geographical patterns of genetic divergence in the widespread Mesoamerican bumble bee *Bombus ephippiatus* (Hymenoptera: Apidae). *Molecular Phylogenetics and Evolution*, **64**, 219–231.
- Ellis, J.S., Knight, M.E., Carvell, C. & Goulson, D. (2006) Cryptic species identification: a simple diagnostic tool for discriminating between two problematic bumblebee species. *Molecular Ecology Notes*, **6**, 540–542.
- Ezra, B.D., Wham, D.C., Hill, C. & Hines, H.M. (2019) Unsupervised machine learning reveals mimicry complexes in bumble bees occur along a perceptual continuum. *Proceedings of the Royal Society of London B*, **286**, 20191501. <https://doi.org/10.1098/rspb.2019.1501>.
- Folmer, O., Black, M., Hoeh, W., Lutz, R. & Vrijenhoek, R. (1994) DNA primers for amplification of mitochondrial cytochrome c oxidase subunit I from diverse metazoan invertebrates. *Molecular Marine Biology and Biotechnology*, **3**, 294–299.
- Fontaneto, D., Flot, J.F. & Tang, C.Q. (2015) Guidelines for DNA taxonomy, with a focus on the meiofauna. *Marine Biodiversity*, **45**, 433–451.
- Frichot, E. & François, O. (2015) LEA: an R package for landscape and ecological association studies. *Methods in Ecology and Evolution*, **6**, 925–929.
- Fujita, M.K., Leaché, A.D., Burbrink, F.T., McGuire, J.A. & Moritz, C. (2012) Coalescent-based species delimitation in an integrative taxonomy. *Trends in Ecology and Evolution*, **27**, 480–488.
- Green, R.E., Krause, J., Briggs, A.W. et al. (2010) A draft sequence of the Neandertal genome. *Science*, **328**, 710–722.
- Handlirsch, A. (1888) Die Hummelsammlung des k. k. naturhistorischen Hofmuseums. *Annalen des Naturhistorischen Museums in Wien*, **3**, 209–250.
- Hebert, P.D.N., Ratnasingham, S. & deWaard, J.R. (2003) Barcoding animal life: cytochrome c oxidase subunit 1 divergences among closely related species. *Proceeding of the Royal Society B*, **270**(suppl), S96–S99.
- Hegland, S.J. & Totland, O. (2008) Is the magnitude of pollen limitation in a plant community affected by pollinator visitation and plant species specialization levels? *Oikos*, **117**, 883–891.
- Hijmans, 2018. raster: Geographic Data Analysis and Modeling. R package version 2.7-15. <https://CRAN.R-project.org/package=raster>
- Hijmans, R.J., Cameron, S.E., Parra, J.L., Jones, P.G. & Jarvis, A. (2005) Very high resolution interpolated climate surfaces for global land areas. *International Journal of Climatology: A Journal of the Royal Meteorological Society*, **25**, 1965–1978.
- Hines, H.M. (2008) Historical biogeography, divergence times, and diversification patterns of bumble bees (Hymenoptera: Apidae: *Bombus*). *Systematic Biology*, **57**, 58–75.
- Hines, H.M. & Williams, P.H. (2012) Mimetic colour pattern evolution in the highly polymorphic *Bombus trifasciatus* (Hymenoptera: Apidae) species complex and its comimics. *Zoological Journal of the Linnean Society*, **166**, 805–826.



- Jackson, J.M., Pimsler, M.L., Oyen, K.J. *et al.* (2018) Distance, elevation and environment as drivers of diversity and divergence in bumble bees across latitude and altitude. *Molecular Ecology*, **27**, 2926–2942. <https://doi.org/10.1111/mec.14735>.
- Kerr, J.T., Pindar, A., Galpern, P. *et al.* (2015) Climate change impacts on bumblebees converge across continents. *Science*, **349**, 177–180.
- Koch, J., Strange, J.P. & Williams, P. (2012) Bumble Bees of the Western United States. A product of the USDA Forest Service Pollinator Partnership, Washington, D.C. and the Pollinator Partnership, San Francisco, California. <https://www.fs.fed.us/wildflowers/pollinators/documents/BumbleBeeGuideWestern2012.pdf>
- Koch, J.B., Rodriguez, J., Pitts, J.P. & Strange, J.P. (2018) Phylogeny and population genetic analyses reveals cryptic speciation in the *Bombus fervidus* species complex (Hymenoptera: Apidae). *PLoS ONE*, **13**, e0207080.
- Kremen, C., Williams, N.M. & Thorp, R.W. (2002) Crop pollination from native bees at risk from agricultural intensification. *Proceedings of the National Academy of Sciences, USA*, **99**, 16812–16816.
- Kumar, S., Stecher, G., Li, M., Knyaz, C. & Tamura, K. (2018) MEGA X: molecular evolutionary genetics analysis across computing platforms. *Molecular Biology & Evolution*, **35**, 1547–1549.
- Lecocq, T., Braseró, N., Martinet, B., Valterová, I. & Rasmont, P. (2015) Highly polytypic taxon complex: interspecific and intraspecific integrative taxonomic assessment of the widespread pollinator *Bombus pascuorum* Scopoli 1763 (Hymenoptera: Apidae). *Systematic Entomology*, **40**, 881–888.
- Li, H. & Durbin, R. (2009) Fast and accurate short read alignment with Burrows-Wheeler Transform. *Bioinformatics*, **25**, 1754–1760.
- Li, H., Handsaker, B., Wysoker, A. *et al.* (2009) The sequence alignment/map format and SAMtools. *Bioinformatics*, **25**, 2078–2079.
- Lozier, J.D. (2014) Revisiting comparisons of genetic diversity in stable and declining species: assessing genome-wide polymorphism in North American bumble bees using RAD sequencing. *Molecular Ecology*, **23**, 788–801.
- Lozier, J.D., Jackson, J.M., Dillon, M.E. & Strange, J.P. (2016a) Population genomics of divergence among extreme and intermediate color forms in a polymorphic insect. *Ecology and Evolution*, **6**, 1075–1091.
- Lozier, J.D., Jackson, J.M., Dillon, M.E. & Strange, J.P. (2016b) Data from: population genomics of divergence among extreme and intermediate colour forms in a polymorphic insect. *Dryad Digital Repository*. <https://doi.org/10.5061/dryad.k21r5>.
- Lozier, J.D., Strange, J.P. & Koch, J.B. (2013) Landscape heterogeneity predicts gene flow in a widespread polymorphic bumble bee, *Bombus bifarius* (Hymenoptera: Apidae). *Conservation Genetics*, **14**, 1099–1110.
- Lozier, J.D., Strange, J.P., Stewart, I.J. & Cameron, S.A. (2011) Patterns of range-wide genetic variation in six North American bumble bee (Apidae: Bombus) species. *Molecular Ecology*, **20**, 4870–4888.
- Malinsky, M., Challis, R.J., Tyers, A.M. *et al.* (2015) Genomic islands of speciation separate cichlid ecomorphs in an East African crater lake. *Science*, **350**, 1493–1498.
- Martin, S.H., Davey, J.W. & Jiggins, C.D. (2015) Evaluating the use of ABBA–BABA statistics to locate introgressed loci. *Molecular Biology and Evolution*, **32**, 244–257.
- Martinet, B., Lecocq, T., Braseró, N. *et al.* (2019) Integrative taxonomy of an arctic bumblebee species complex highlights a new cryptic species (Apidae: Bombus). *Zoological Journal of the Linnean Society*, **187**, 599–621.
- May, R.M. (1988) How many species are there on earth? *Science*, **241**, 1441–1449.
- Mayr, E. (1961) Cause and effect in biology. *Science*, **134**, 1501–1506.
- McKenna, A., Hanna, M., Banks, E. *et al.* (2010) The Genome Analysis Toolkit: a MapReduce framework for analyzing next-generation DNA sequencing data. *Genome Research*, **20**, 1297–1303.
- Memmott, J., Waser, N.M. & Price, M.V. (2004) Tolerance of pollination networks to species extinctions. *Proceeding of the Royal Society B*, **271**, 2605–2611.
- Michener, C.D. (2000) *The Bees of the World*. Johns Hopkins Press, Baltimore, MD.
- Murray, T.E., Fitzpatrick, Ú., Brown, M.J.F. & Paxton, R.J. (2008) Cryptic species diversity in a widespread bumble bee complex revealed using mitochondrial DNA RFLPs. *Conservation Genetics*, **9**, 653–666.
- Owen, R.E. & Plowright, R.C. (1980) Abdominal pile color dimorphism in the bumble bee, *Bombus melanopygus*. *Journal of Heredity*, **71**, 241–247.
- Pardo-Díaz, C., Salazar, C., Baxter, S.W. *et al.* (2012) Adaptive introgression across species boundaries in *Heliconius* butterflies. *PLoS Genetics*, **8**, e1002752.
- Pfenninger, M. & Schwenk, K. (2007) Cryptic animal species are homogeneously distributed among taxa and biogeographical regions. *BMC Evolutionary Biology*, **7**, 121.
- Phillips, S.J. & Dudík, M. (2008) Modeling of species distributions with Maxent: new extensions and a comprehensive evaluation. *Ecography*, **31**, 161–175.
- Phillips, S.J., Dudík, M. & Schapire, R.E. (2004) A maximum entropy approach to species distribution modeling. *Proceedings of the 21st International Conference on Machine Learning*, pp. 655–662. ACM Press, New York, NY.
- Phillips, S.J., Dudík, M. & Schapire, R.E. (2017) Maxent software for modeling species niches and distributions v. 3.4.1 [WWW document]. URL [http://biodiversityinformatics.amnh.org/open\\_source/maxent](http://biodiversityinformatics.amnh.org/open_source/maxent) [accessed in 2017].
- Pimsler, M.L., Jackson, J.M. & Lozier, J.D. (2017) Population genomics reveals a candidate gene involved in bumble bee pigmentation. *Ecology and Evolution*, **7**, 3406–3413.
- Rambaut, A., Drummond, A.J., Xie, D., Baele, G. & Suchard, M.A. (2018) Posterior summarisation in Bayesian phylogenetics using Tracer 1.7. *Systematic Biology*, **67**, 901–904.
- Rasmont, P., Franzén, M., Lecocq, T. *et al.* (2015) Climatic risk and distribution Atlas of european bumblebees. *BioRisk*, **10**, 1–246.
- Rasmont, P., Terzo, M., Aytikin, A.M. *et al.* (2005) Cephalic secretions of the bumble bee subgenus *Sibiricobombus* Vogt suggest *Bombus niveatus* Kriechbaumer and *Bombus vorticoides* Gerstaecker are conspecific (Hymenoptera, Apidae, Bombus). *Apidologie*, **36**, 571–584.
- Ronquist, F. & Huelsenbeck, J.P. (2003) MrBayes 3: Bayesian phylogenetic inference under mixed models. *Bioinformatics*, **19**, 1572–1574.
- Runemark, A., Trier, C.N., Eroukhanoff, F. *et al.* (2018) Variation and constraints in hybrid genome formation. *Nature Ecology & Evolution*, **2**, 549–556.
- Sadd, B.M., Barribeau, S.M., Bloch, G. *et al.* (2015) The genomes of two key bumblebee species with primitive eusocial organization. *Genome Biology*, **16**, 76.
- Stephen, W.P. (1957) *Bumble Bees of Western America (Hymenoptera: Apoidea)*. Technical Bulletin 40. Agricultural Experiment Station, Oregon State College, Corvallis, OR.
- Thorp, R.W., Horning, D.S. & Dunning, L.L. (1983) Bumble bees and cuckoo bumble bees of California (Hymenoptera: Apidae). *Bulletin of the California Insect Survey*, **23**, 1–79.
- Tian, L., Rahman, S.R., Ezray, B.D., Franzini, L., Strange, J.P., Lhomme, P. & Hines, H.M. (2019) A homeotic shift late in development drives mimetic color variation in a bumble bee. *Proceedings of the National Academy of Sciences*, **116**, 11857–11865.

- Van Belleghem, S.M., Rastas, P., Papanicolaou, A. *et al.* (2017) Complex modular architecture around a simple toolkit of wing pattern genes. *Nature Ecology & Evolution*, **1**, 0052.
- Van der Auwera, G.A., Carneiro, M.O., Hartl, C. *et al.* (2013) From FastQ data to high-confidence variant calls: the genome analysis toolkit best practices pipeline. *Current Protocols in Bioinformatics*, **43**, 11.10.1–11.10.33.
- Velthuis, H.H.W. & Van Doorn, A. (2006) A century of advances in bumble bee domestication and the economic and environmental aspects of its commercialization for pollination. *Apidologie*, **37**, 421–451.
- Wickham, H. (2016) *ggplot2: Elegant Graphics for Data Analysis*. Springer, New York, NY.
- Williams, P.H. (1998) An annotated checklist of bumble bees with an analysis of patterns of description (Hymenoptera: Apidae, Bombini). *Bulletin of the Natural History Museum of London*, **67**, 79–152.
- Williams, P.H. (2007) The distribution of bumble bee colour patterns worldwide: possible significance for thermoregulation, crypsis and warning mimicry. *Biological Journal of the Linnaen Society*, **92**, 97–118.
- Williams, P.H., Berezin, M.V., Cannings, S.G. *et al.* (2019). The arctic and alpine bumblebees of the subgenus *Alpinobombus* revised from integrative assessment of species' gene coalescents and morphology (Hymenoptera, Apidae, Bombus). *Zootaxa*, **4625**, 1–68.
- Williams, P.H., Brown, M.J.F., Carolan, J.C. *et al.* (2012) Unveiling cryptic species of the bumble bee subgenus *Bombus s. str.* worldwide with COI barcodes (Hymenoptera: Apidae). *Systematics and Biodiversity*, **10**, 21–56.
- Williams, P.H., Huang, J., Rasmont, P. & An, J. (2016) Early-diverging bumblebees from across the roof of the world: the high-mountain subgenus *Mendacibombus* revised from species' gene coalescents and morphology (Hymenoptera, Apidae). *Zootaxa*, **4204**, 1–72.
- Williams, P.H., Ito, M., Matsumura, T. & Kudo, I. (2010) The bumblebees of the Nepal Himalaya (Hymenoptera: Apidae). *Insecta Matsumurana*, **66**, 115–151.
- Williams, P.H. & Osborne, J.L. (2009) Bumble bee vulnerability and conservation world-wide. *Apidologie*, **40**, 367–387.
- Williams, P.H., Thorp, R.W., Richardson, L.L. & Colla, S.R. (2014) *Bumble Bees of North America: An Identification Guide*. Princeton University Press, Princeton, NJ.
- Woodard, S.H., Lozier, J.D., Goulson, D. *et al.* (2015) Molecular tools and bumble bees: revealing hidden details of ecology and evolution in a model system. *Molecular Ecology*, **24**, 2916–2936. <https://doi.org/10.1111/mec.13198>.
- Zhang, J.J., Kapli, P., Pavlidis, P. & Stamatakis, A. (2013) A general species delimitation method with applications to phylogenetic placements. *Bioinformatics*, **29**, 2869–2876.

Accepted 6 December 2019